Mechanical Sensorless Speed Control of Permanent-Magnet AC Motors Driving an Unknown Load

Cristian De Angelo, *Member, IEEE*, Guillermo Bossio, Jorge Solsona, *Senior Member, IEEE*, Guillermo O. García, *Senior Member, IEEE*, and María Inés Valla, *Senior Member, IEEE*

***Abstract*—A new sensorless scheme for high-performance speed control of permanent-magnet ac motors (PMACMs) driving an unknown load is proposed. This scheme uses an extended nonlinear reduced-order observer to estimate the induced electromotive force (EMF) and load torque. From the estimated variables, the rotor position, the rotor speed, and the position derivative of flux are calculated and are used to close the control loop. In order to improve the drive performance, the estimated load torque is incorporated as a feedforward signal in the closed control loop. In addition, the proposed sensorless PMACM drive allows the torque-ripple and copper-loss minimization for motors with an arbitrary EMF waveform. Simulation and experimental results to validate the proposal are presented in this paper.**

***Index Terms*—Nonlinear estimation, nonsinusoidal electromotive-force (EMF) waveform, permanent-magnet motors, unknown load torque estimation.**

I. Introduction

PERMANENT-MAGNET ac motor (PMACM) drives are widely used in high-performance applications. These machines are preferred because of the absence of rotor windings and brushes, the high efficiency, and the power density. Several techniques, such as vector control, feedback linearization, and other nonlinear methods have been proposed to obtain an accurate speed and torque control. However, an important requirement of high-performance applications is the drive robustness against disturbance torques like load changes or mechanical parameter variations. This leads to the necessity of a compensation for the disturbance torque. Unfortunately, the disturbance torque cannot be easily measured or predicted [1]–[4].

Different proposals use extended-state full-order observers [3] or disturbance observers [4] to estimate the disturbance torque and implement a nonlinear speed control through feedback linearization. However, to implement these techniques, a mechanical sensor is needed. This sensor increases costs and reduces the drive reliability. This has led to the research and development of some methods of PMACM control avoiding those sensors [5]. Other techniques have been proposed for different machines [2], [6], [7].

Another important requirement for high-performance applications is a ripple-free torque control. Several techniques have been proposed for minimizing torque pulsations produced by nonsinusoidal electromotive-force (EMF) waveforms [8]. The most common techniques are based on the active control of the excitation currents for obtaining current waveforms synchronized with the rotor position. In this way, it is possible to cancel the harmonic torque components. In order to implement the torque-ripple-minimization strategies without the use of a position sensor, an observer that takes into account nonsinusoidal EMF waveforms is needed.

In this paper, a new sensorless strategy for speed control of PMACMs is proposed. Assuming that an unknown load is driven by the machine, an extended nonlinear reduced-order observer is used to estimate the induced EMF and load torque. From the estimated variables, the rotor position, the rotor speed, and the position derivative of flux are calculated and are used to close the control loop.

In order to improve the drive performance, the estimated load torque is incorporated as a feedforward signal in the speed control loop. In addition, since the proposed observer includes information about the machine's EMF waveform, it allows the torque-ripple and copper-loss minimization, for motors with any EMF waveform. In this way, a high-performance sensorless PMACM drive is obtained.

This paper is organized as follows. The PMACM general model is presented first. Then, the proposed observer is developed; after that, the observer is used in a sensorless speed control strategy, with feedforward torque compensation, to implement a complete PMACM drive. Simulation and

Manuscript received June 30, 2004; revised January 6, 2005. Abstract published on the Internet January 25, 2006. This work was supported in part by the Universidad Nacional de Río Cuarto (UNRC), in part by the Universidad Nacional de La Plata (UNLP), in part by the Universidad Nacional del Sur, in part by the FONCyT-ANPCyT, and in part by the Consejo Nacional de Investigaciones Científicas y Técnicas (CONICET). An earlier version of this paper was presented at the IEEE International Symposium on Industrial Electronics, Rio de Janeiro, Brazil, June 9–12, 2003.

C. De Angelo, G. Bossio, and G. O. García are with the Consejo Nacional de Investigaciones Científicas y Técnicas (CONICET), Argentina, and also with the Grupo de Electrónica Aplicada (GEA), Facultad de Ingeniería, Universidad Nacional de Río Cuarto, X5804BYA Río Cuarto, Argentina (e-mail: cdeangelo@ieee.org; gbossio@ing.unrc.edu.ar; g.garcia@ieee.org).

J. Solsona is with the Consejo Nacional de Investigaciones Científicas y Técnicas (CONICET), Argentina, and also with the Departamento de Ingeniería Eléctrica y de Computadoras, Instituto de Investigaciones en Ingeniería Eléctrica "Alfredo Desages," Universidad Nacional del Sur, 8000 Bahía Blanca, Argentina (e-mail: jsolsona@uns.edu.ar).

M. I. Valla is with the Consejo Nacional de Investigaciones Científicas y Técnicas (CONICET), Argentina, and also with the Laboratorio de Electrónica Industrial, Control e Instrumentación (LEICI), Departamento de Electrotecnia, Facultad de Ingeniería, Universidad Nacional de La Plata, 1900 La Plata, Argentina (e-mail: m.i.valla@ieee.org).

Digital Object Identifier 10.1109/TIE.2006.870723

experimental results of the whole system are included. Finally, conclusions are drawn.

II. PMACM Model

In order to develop the proposed observer, the dynamic model of a PMACM can be written in a stationary reference frame $\alpha\beta$ [9]

$$\begin{aligned}\frac{di_\alpha}{dt} &= -\frac{R}{L}i_\alpha - \frac{1}{L}e_\alpha + \frac{1}{L}v_\alpha \\ \frac{di_\beta}{dt} &= -\frac{R}{L}i_\beta - \frac{1}{L}e_\beta + \frac{1}{L}v_\beta \end{aligned} \tag{1}$$

$$\begin{aligned}\frac{d\theta}{dt} &= \omega \\ \frac{d\omega}{dt} &= \frac{1}{J}T_e - \frac{1}{J}T_L \end{aligned} \tag{2}$$

where i_α, i_β, e_α, e_β, v_α, and v_β represent the current, the induced-EMF, and the excitation-voltage components, respectively; R and L are the stator resistance and inductance, respectively; θ, ω, and T_e represent the rotor position and speed and the electromagnetic torque produced by the machine; J and T_L are the inertia and the load torque, respectively. Viscosity B is considered as part of the unknown load torque.

The EMF induced into the stator windings is given by

$$\begin{aligned}e_\alpha &= \frac{\partial \lambda_\alpha}{\partial \theta}\frac{d\theta}{dt} = \varphi_\alpha(\theta)\omega \\ e_\beta &= \frac{\partial \lambda_\beta}{\partial \theta}\frac{d\theta}{dt} = \varphi_\beta(\theta)\omega \end{aligned} \tag{3}$$

where λ_α and λ_β are the linked flux components and φ_α and φ_β are the components of the flux derivative with respect to the rotor position.

In a sinusoidal PMACM, φ_α and φ_β are sinusoidal functions of the position; whereas, in trapezoidal PMACMs, they are trapezoidal. However, in many PMACMs, these functions are neither sinusoidal nor trapezoidal. For this reason, φ_α and φ_β are functions to be determined according to the motor type. These functions can be previously determined in an experimental way by measuring the instantaneous voltage, the rotor position, and the speed under no-load condition or by means of a self-commissioning scheme, as proposed in [10]. To include these waveforms in the PMACM model, a Fourier-series approximation is used in this paper. In this way, the EMF estimation is enhanced.

Employing a more accurate model for the EMF waveforms, it is possible to improve the observer-based controller performance. The $\alpha\beta$ components of the position derivative of flux can be represented using Fourier series as follows [11]:

$$\begin{aligned}\varphi_\alpha(\theta) &= \sum_{n=1}^{\infty} -\Phi_{(2n-1)}\sin\left((2n-1)\theta\right) \\ \varphi_\beta(\theta) &= \sum_{n=1}^{\infty} \Phi_{(2n-1)}\cos\left((2n-1)\theta\right) \end{aligned} \tag{4}$$

where $\Phi_{(2n-1)}$ is the magnitude of the $(2n-1)$ harmonic.

The electromagnetic torque in the last equation of (2) can be represented by [9]

$$T_e = \varphi_\alpha(\theta)i_\alpha + \varphi_\beta(\theta)i_\beta. \tag{5}$$

Thus, it is evident that the excitation current waveforms greatly depend on the functions φ_α and φ_β in order to obtain a smooth controlled torque.

The model presented in this section is not limited to sinusoidal or trapezoidal PMACMs as previous proposals do. Based on this model, an extended nonlinear reduced-order observer to estimate the induced EMF, the rotor position, the rotor speed, and the load torque for arbitrary-EMF-waveform PMACMs is introduced in the next section.

III. Extended Nonlinear Reduced-Order Observer

In order to obtain rotor position, the rotor speed, and an unknown load torque, an extended nonlinear reduced-order observer is proposed. This observer estimates the induced EMF and load torque. Then, the estimated EMF is used for reconstructing the rotor speed, the rotor position, and the position derivative of flux. The observer is designed as follows. The time derivative of EMF can be calculated from (3)

$$\begin{aligned}\frac{de_\alpha}{dt} &= \frac{d\varphi_\alpha}{dt}\omega + \varphi_\alpha\frac{d\omega}{dt} \\ \frac{de_\beta}{dt} &= \frac{d\varphi_\beta}{dt}\omega + \varphi_\beta\frac{d\omega}{dt} \end{aligned} \tag{6}$$

where the speed time derivative can be replaced from (2) and (5), obtaining

$$\begin{aligned}\frac{de_\alpha}{dt} &= \frac{d\varphi_\alpha}{dt}\omega + \frac{1}{J}\varphi_\alpha(\varphi_\alpha i_\alpha + \varphi_\beta i_\beta) - \frac{1}{J}\varphi_\alpha T_L \\ \frac{de_\beta}{dt} &= \frac{d\varphi_\beta}{dt}\omega + \frac{1}{J}\varphi_\beta(\varphi_\alpha i_\alpha + \varphi_\beta i_\beta) - \frac{1}{J}\varphi_\beta T_L. \end{aligned} \tag{7}$$

Since the load is unknown, a slowly variant load torque, slower than the system dynamics, is assumed. This assumption covers the majority of the application cases. Then, a new state is included to estimate the unknown load torque, as follows:

$$\frac{dT_L}{dt} \approx 0. \tag{8}$$

In such a case, the following extended reduced-order observer is proposed:

$$\begin{aligned}\frac{d\widehat{e}_\alpha}{dt} &= \frac{d\widehat{\varphi}_\alpha}{dt}\widehat{\omega} + \frac{1}{J}\widehat{\varphi}_\alpha(\widehat{\varphi}_\alpha i_\alpha + \widehat{\varphi}_\beta i_\beta) \\ &\quad - \frac{1}{J}\widehat{\varphi}_\alpha\widehat{T}_L + g\left(L\frac{d\widehat{i}_\alpha}{dt} - L\frac{di_\alpha}{dt}\right) \\ \frac{d\widehat{e}_\beta}{dt} &= \frac{d\widehat{\varphi}_\beta}{dt}\widehat{\omega} + \frac{1}{J}\widehat{\varphi}_\beta(\widehat{\varphi}_\alpha i_\alpha + \widehat{\varphi}_\beta i_\beta) \\ &\quad - \frac{1}{J}\widehat{\varphi}_\beta\widehat{T}_L + g\left(L\frac{d\widehat{i}_\beta}{dt} - L\frac{di_\beta}{dt}\right) \\ \frac{d\widehat{T}_L}{dt} &= l_a \end{aligned} \tag{9}$$

where $\widehat{x}$ is the estimated value of x, g is a constant gain, and l_a is the adaptation law to be determined to obtain the desired convergence of the estimated load torque (see the Appendix) as

$$l_a = -\frac{\Gamma L}{J}\left[\widehat{\varphi}_\alpha\left(\frac{d\widehat{i}_\alpha}{dt} - \frac{di_\alpha}{dt}\right) + \widehat{\varphi}_\beta\left(\frac{d\widehat{i}_\beta}{dt} - \frac{di_\beta}{dt}\right)\right] \quad (10)$$

where Γ is a constant gain.

In this reduced-order observer, the time derivatives of stator currents are used as correction terms. The estimated current derivatives, necessary for obtaining the correction term, can be calculated with (1) as

$$\begin{aligned}\frac{d\widehat{i}_\alpha}{dt} &= -\frac{R}{L}i_\alpha - \frac{1}{L}\widehat{e}_\alpha + \frac{1}{L}v_\alpha \\ \frac{d\widehat{i}_\beta}{dt} &= -\frac{R}{L}i_\beta - \frac{1}{L}\widehat{e}_\beta + \frac{1}{L}v_\beta.\end{aligned} \quad (11)$$

The estimate of the machine's speed can be found by taking into account (3), thus

$$e_\alpha^2 + e_\beta^2 = \omega^2\left(\varphi_\alpha^2 + \varphi_\beta^2\right) \quad (12)$$

and

$$\widehat{\omega} = \sqrt{\frac{\widehat{e}_\alpha^2 + \widehat{e}_\beta^2}{\widehat{\varphi}_\alpha^2 + \widehat{\varphi}_\beta^2}}. \quad (13)$$

As can be seen, it is not possible to determine the sign of the estimated speed from the last equation. However, it can be modified by obtaining the estimated speed sign from an approximation of the time derivative of the estimated position (see [11]). Then, the estimated speed is calculated as

$$\widehat{\omega} = \operatorname{sign}\left(\frac{\Delta\widehat{\theta}}{\Delta t}\right)\sqrt{\frac{\widehat{e}_\alpha^2 + \widehat{e}_\beta^2}{\widehat{\varphi}_\alpha^2 + \widehat{\varphi}_\beta^2}} \quad (14)$$

where $\widehat{\theta}$ is given in (18).

The calculation of the time derivative of the measured current, used in the correction terms (9) and (10), may end up in a noisy estimation. To avoid this, the following change of variables is proposed:

$$\begin{aligned}\zeta_\alpha &= \widehat{e}_\alpha + gLi_\alpha \\ \zeta_\beta &= \widehat{e}_\beta + gLi_\beta \\ \tau &= \widehat{T}_L - \frac{\Gamma L}{J}(\widehat{\varphi}_\alpha i_\alpha + \widehat{\varphi}_\beta i_\beta).\end{aligned} \quad (15)$$

The dynamic equations to be implemented are obtained by differentiating (15) with respect to time and substituting from (9), (10), and (13). These equations become

$$\begin{aligned}\frac{d\zeta_\alpha}{dt} &= \frac{d\widehat{\varphi}_\alpha}{dt}\sqrt{\frac{\widehat{e}_\alpha^2 + \widehat{e}_\beta^2}{\widehat{\varphi}_\alpha^2 + \widehat{\varphi}_\beta^2}} + \frac{1}{J}\widehat{\varphi}_\alpha(\widehat{\varphi}_\alpha i_\alpha + \widehat{\varphi}_\beta i_\beta) \\ &\quad - \frac{1}{J}\widehat{\varphi}_\alpha\widehat{T}_L + gL\frac{d\widehat{i}_\alpha}{dt} \\ \frac{d\zeta_\beta}{dt} &= \frac{d\widehat{\varphi}_\beta}{dt}\sqrt{\frac{\widehat{e}_\alpha^2 + \widehat{e}_\beta^2}{\widehat{\varphi}_\alpha^2 + \widehat{\varphi}_\beta^2}} + \frac{1}{J}\widehat{\varphi}_\beta(\widehat{\varphi}_\alpha i_\alpha + \widehat{\varphi}_\beta i_\beta) \\ &\quad - \frac{1}{J}\widehat{\varphi}_\beta\widehat{T}_L + gL\frac{d\widehat{i}_\beta}{dt} \\ \frac{d\tau}{dt} &= -\frac{\Gamma L}{J}\left(\widehat{\varphi}_\alpha\frac{d\widehat{i}_\alpha}{dt} + \widehat{\varphi}_\beta\frac{d\widehat{i}_\beta}{dt} + \frac{d\widehat{\varphi}_\alpha}{dt}i_\alpha + \frac{d\widehat{\varphi}_\beta}{dt}i_\beta\right)\end{aligned} \quad (16)$$

and the estimated EMF and load torque can be obtained from (15) as

$$\begin{aligned}\widehat{e}_\alpha &= \zeta_\alpha - gLi_\alpha \\ \widehat{e}_\beta &= \zeta_\beta - gLi_\beta \\ \widehat{T}_L &= \tau + \frac{\Gamma L}{J}(\widehat{\varphi}_\alpha i_\alpha + \widehat{\varphi}_\beta i_\beta).\end{aligned} \quad (17)$$

The proposed extended observer can be applied to any PMACM, independently of its EMF waveform. The only requirement for its implementation is to know the waveforms of the flux derivative with respect to the rotor position. These functions are incorporated in the observer by evaluating (4) in the estimated rotor position. Taking into account that the EMF waveform has several harmonic components, the estimated position can be calculated from the EMF fundamental, using

$$\widehat{\theta} = \tan^{-1}\left(\frac{-\widehat{e}_{\alpha 1}}{\widehat{e}_{\beta 1}}\right) \quad (18)$$

where $e_{\alpha 1}$ and $e_{\beta 1}$ are the induced-EMF-waveform fundamental components, which can be obtained by eliminating the harmonic components, as proposed in [12]. These harmonic components can be calculated at sample (k) from the Fourier-series approximation (4), evaluated in an approximation of the current position $\widetilde{\theta}_{(k)}$. In order to do that, a constant speed between two consecutive samples is considered, then

$$\begin{aligned}\widetilde{e}_{\alpha h(k)} &= \widehat{\omega}_{(k-1)}\sum_{n=2}^{\infty} -\Phi_{(2n-1)}\sin\left((2n-1)\widetilde{\theta}_{(k)}\right) \\ \widetilde{e}_{\beta h(k)} &= \widehat{\omega}_{(k-1)}\sum_{n=2}^{\infty} \Phi_{(2n-1)}\cos\left((2n-1)\widetilde{\theta}_{(k)}\right)\end{aligned} \quad (19)$$

where $\widetilde{e}_{\alpha h(k)}$ and $\widetilde{e}_{\beta h(k)}$ are the harmonic components of the estimated EMF (note that the sum is taken from $n = 2$).

The approximation of the current position is obtained considering the speed as

$$\widetilde{\omega} = \frac{\theta_{(k)} - \theta_{(k-1)}}{T_s} \quad (20)$$

in a sample time T_s, thus

$$\widetilde{\theta}_{(k)} = \widehat{\theta}_{(k-1)} + \widehat{\omega}_{(k-1)}T_s. \quad (21)$$

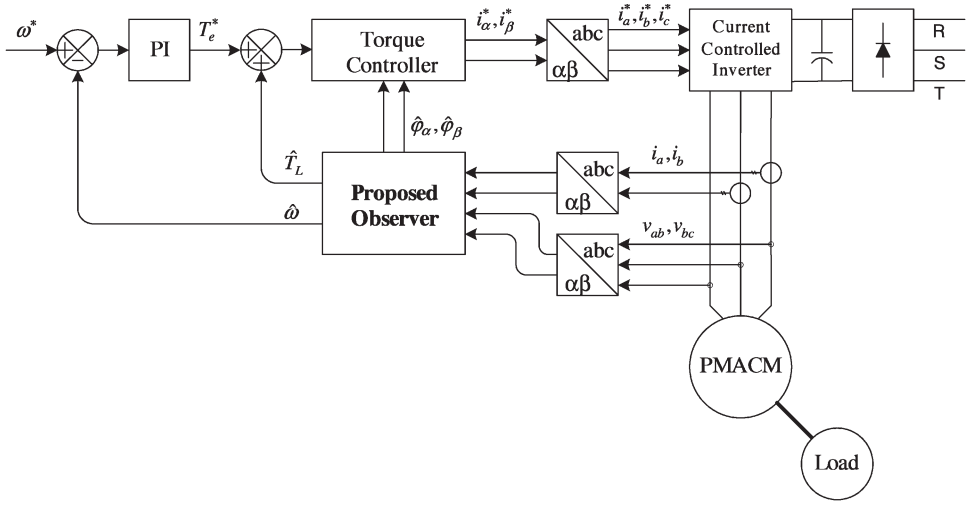

Fig. 1. Scheme of the proposed sensorless speed control drive with feedforward load torque compensation.

Then, the induced-EMF fundamental components can be calculated subtracting the harmonic components (19) from the EMF estimated by the observer as

$$\begin{aligned}\widehat{e}_{\alpha 1} &= \widehat{e}_{\alpha} - \widetilde{e}_{\alpha h(k)} \\ \widehat{e}_{\beta 1} &= \widehat{e}_{\beta} - \widetilde{e}_{\beta h(k)}\end{aligned} \tag{22}$$

and the new estimated position is calculated from (18). Then, according to (4), the estimated position derivative of flux is calculated as

$$\begin{aligned}\widehat{\varphi}_{\alpha}(\widehat{\theta}) &= \sum_{n=1}^{\infty} -\Phi_{(2n-1)} \sin\left((2n-1)\widehat{\theta}\right) \\ \widehat{\varphi}_{\beta}(\widehat{\theta}) &= \sum_{n=1}^{\infty} \Phi_{(2n-1)} \cos\left((2n-1)\widehat{\theta}\right)\end{aligned} \tag{23}$$

and their estimated time derivatives can be calculated as

$$\begin{aligned}\frac{d\widehat{\varphi}_{\alpha}}{dt} &= \widehat{\omega} \sum_{n=1}^{\infty} -(2n-1)\Phi_{(2n-1)} \cos\left((2n-1)\widehat{\theta}\right) \\ \frac{d\widehat{\varphi}_{\beta}}{dt} &= \widehat{\omega} \sum_{n=1}^{\infty} -(2n-1)\Phi_{(2n-1)} \sin\left((2n-1)\widehat{\theta}\right)\end{aligned} \tag{24}$$

which completes the proposed observer for PMACMs with arbitrary EMF waveforms.

It must be noted that nonlinear reduced-order observers in combination with load torque estimators cannot be found in literature, to the best knowledge of the authors. Also, it must be remarked that there exist two main advantages obtained with the use of this kind of observer. One advantage is the improvement of the observer transient performance in comparison with a nonlinear full-order observer. The other advantage is the diminished steady-state EMF estimation error resulting from the use of the unknown load torque estimator. Consequently, since both transient and steady-state observer performances are improved, the mechanical sensorless speed control is improved as well.

IV. Sensorless Speed Control With Feedforward Torque Compensation

Fig. 1 shows the proposed mechanical sensorless PMACM drive with feedforward load torque compensation. This scheme is composed of an internal torque control loop and an external speed control loop. In order to compensate for the disturbance torque, the estimated load torque is added to the torque reference as a feedforward compensation in the speed control loop.

The technique for motor torque control proposed in [13] is used in this paper. According to Leidhold *et al.* [13], the current references needed for torque control can be obtained by applying the theory of the instantaneous reactive power [14]. Therefore, the current references can be expressed as follows:

$$\begin{aligned}i_{\alpha}^{*} &= \frac{\left(T_e^{*} + \widehat{T}_L\right)\widehat{\varphi}_{\alpha}}{\widehat{\varphi}_{\alpha}^2 + \widehat{\varphi}_{\beta}^2} \\ i_{\beta}^{*} &= \frac{\left(T_e^{*} + \widehat{T}_L\right)\widehat{\varphi}_{\beta}}{\widehat{\varphi}_{\alpha}^2 + \widehat{\varphi}_{\beta}^2}\end{aligned} \tag{25}$$

where the estimated variables obtained from the observer are used to close the control loops.

The proposed strategy was implemented to control the speed of an experimental prototype of axial-flux PMACM, available at the Grupo de Electrónica Aplicada, Universidad Nacional de Río Cuarto (GEA-UNRC) Laboratory. The motor parameters are as follows:

three-phase axial-flux permanent-magnet motor, 16 poles, 4000 r/min, 30 kW;
$R = 10$ mΩ;
$L = 100$ μH;
$J = 0.78$ kg $\cdot$ m^2;
$B = 0.0015$ kg $\cdot$ m^2/s;
$\Phi_1 = 0.5021$ and $\Phi_5 = \Phi_1/25$ (harmonics of the Fourier-series approximation).

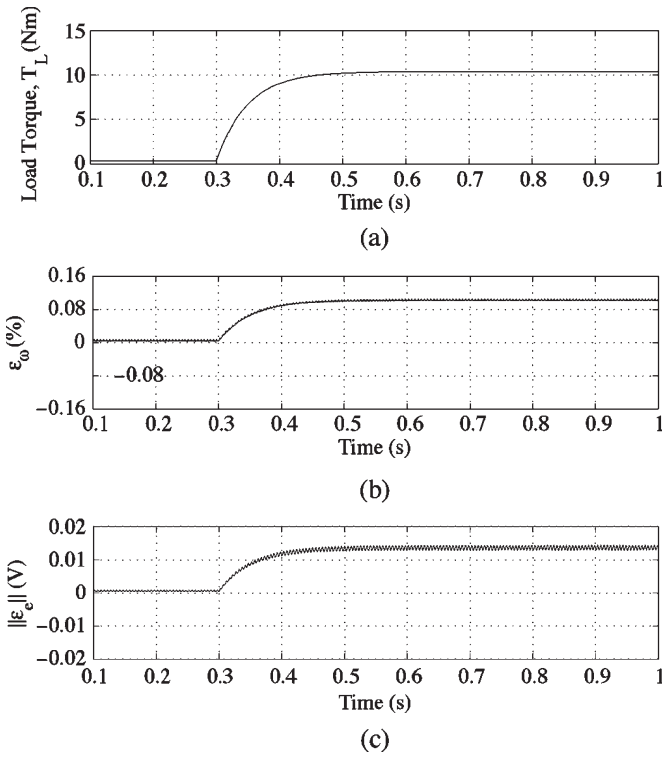

Fig. 2. Estimation error without load torque compensation. (a) Applied load torque T_L. (b) Speed estimation error ε_ω. (c) Norm of the EMF estimation error $\|\varepsilon_e\|$.

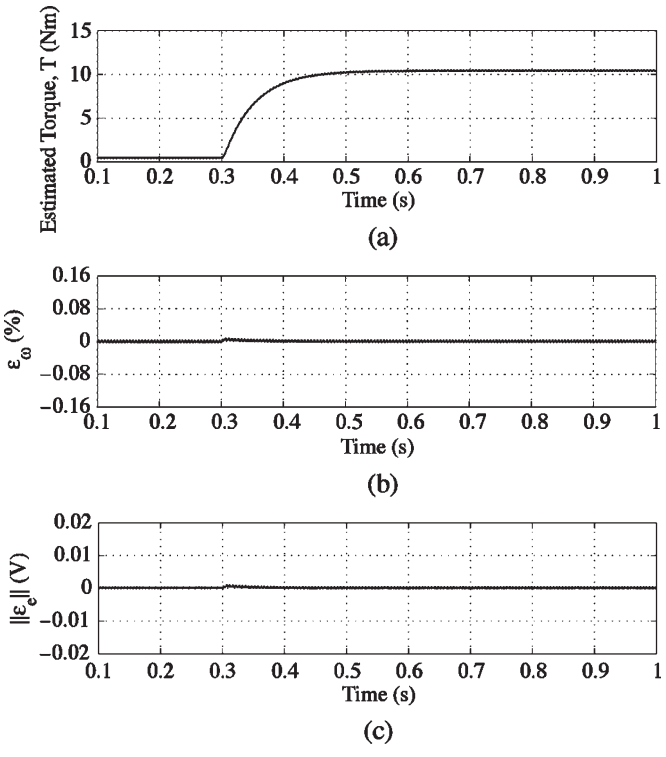

Fig. 3. Estimation error with load torque compensation. (a) Estimated load torque $\widehat{T}_L$. (b) Speed estimation error ε_ω. (c) Norm of the EMF estimation error $\|\varepsilon_e\|$.

Observer gains were set at $g = 400$ and $\Gamma = 10\,000$. Simulations and experimental results were obtained to validate the proposal.

A. Simulation Results

Since the motor EMF cannot be measured, numerical simulations were performed in order to show the improvement in the EMF estimation convergence when the proposed strategy is used, when compared with an observer without load torque compensation [11].

Results obtained from the observer without compensation are shown in Fig. 2, while Fig. 3 shows the results of the observer employing the proposed load torque compensation. For both figures, the PMACM is driven unloaded at 250 r/min, when the load torque shown in Fig. 2(a) is applied.

Fig. 2(b) shows the speed estimation error ($\varepsilon_\omega = \omega - \widehat{\omega}$), when the cited load is applied. As can be seen, the speed estimation error remains at a constant nonzero value when the load torque is not compensated. The same occurs with the norm of the EMF estimation error [Fig. 2(c)].

Fig. 3(a) shows the estimated load torque, using the proposed adaptation law. In Fig. 3(b) and (c), the speed estimation error and the norm of the EMF estimation error are shown. As can be seen, the estimation errors approach zero immediately when the proposed compensation is used. As a conclusion, the load torque estimation improves the observer convergence.

Since viscosity was taken as a part of the unknown load torque, this perturbation is also estimated by the proposed observer, as shown in Fig. 4. Fig. 4(a) shows the machine speed,

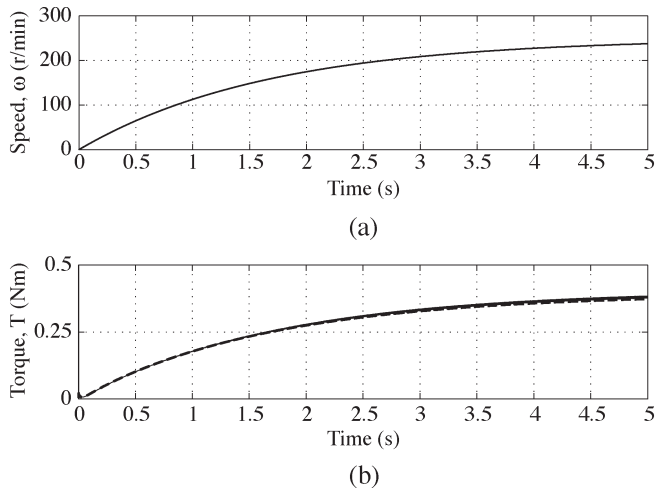

Fig. 4. Estimation of viscosity $B\omega$. (a) Unloaded machine speed ω. (b) $B\omega$ disturbance (dashed line) and estimated load torque $\widehat{T}_L$ (solid line).

when it is driven unloaded from rest. The estimation of $B\omega$ is shown in Fig. 4(b); the actual one is shown by a dashed line and the estimated one is shown by a solid line.

Simulations of the complete system were performed in order to evaluate its performance. The simulated operation condition corresponds to the machine driven at 300-r/min constant speed, when a 5-N·m load torque is applied. A great improvement in the system response can be observed when using the load torque compensation. This can be seen in Fig. 5, where the speed tracking error (difference between reference speed and actual speed, ε_ω^*) is shown, without load torque compensation

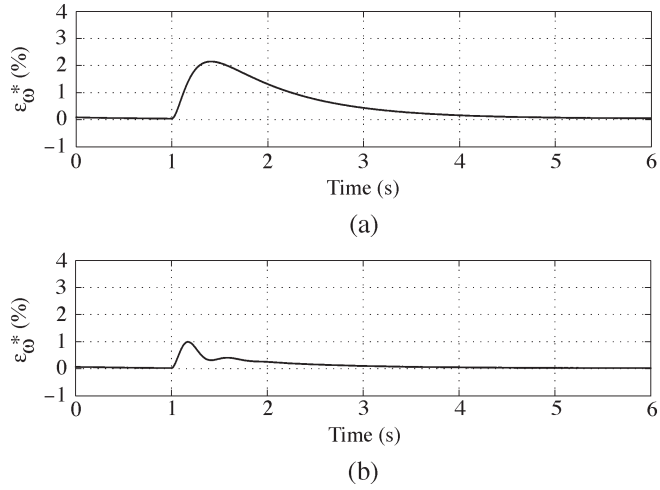

Fig. 5. Speed tracking error ε_ω^* (a) without load torque compensation and (b) with load torque compensation.

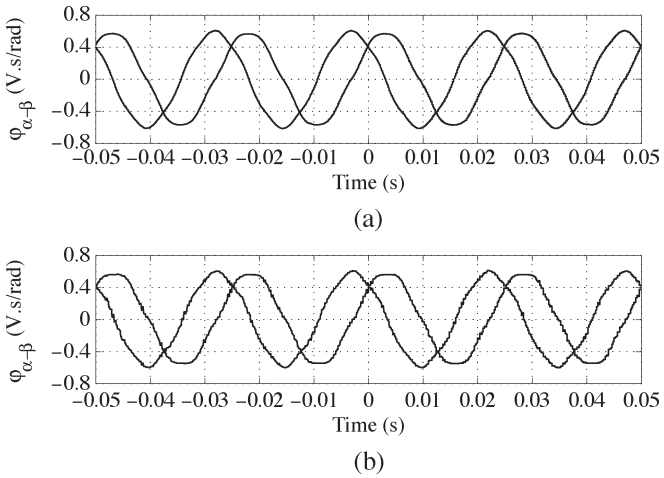

Fig. 6. Position derivative of linked flux at low speed. (a) Measured: φ_α, φ_β. (b) Estimated: $\widehat{\varphi}_\alpha$, $\widehat{\varphi}_\beta$.

[Fig. 5(a)] and with load torque compensation [Fig. 5(b)]. Thus, the proposed load torque estimation improves the observer convergence and allows the implementation of a feedforward torque compensation.

B. Experimental Results

Experimental results evaluating the proposed sensorless drive performance are presented here. Since low speed is the more critical situation for sensorless drives, all the tests presented in this section use speeds below 0.1 per unit (p.u.). The axial-flux PMACM is driven by a pulsewidth-modulated inverter with a fast current control loop, available at the GEA-UNRC Laboratory. The observer and the control algorithm were implemented on a PC with a QNX real-time platform, programmed in C++ language. Differential equations were discretized using the second-order Runge–Kutta method with a sampling period equal to 180 μs. Motor voltages and currents were measured using standard Hall effect sensors and acquired by means of 12-bit A/D converters. The actual motor speed was measured with the only purpose of showing the estimation errors. The estimated variables are always used in the control loops.

Fig. 6 shows the approximation of the position derivative of the flux. Fig. 6(b) presents the Fourier-series approximation of the position derivative of flux in $\alpha\beta$ coordinates, when the motor runs at a low speed of 300 r/min (0.075 p.u.). The waveforms shown here approximate very well the actual ones presented in Fig. 6(a), which were previously obtained and stored in a lookup table.

The position estimation at low speed is shown in Fig. 7. In Fig. 7(a), the actual rotor position at 100 r/min (0.025 p.u.) is shown. The estimated position is shown in Fig. 7(b), while the estimation position error ($\varepsilon_\theta = \theta - \widehat{\theta}$) is presented in Fig. 7(c).

Fig. 8 shows the system response when the machine is driven at a 300-r/min constant speed and a 5-N·m load torque is applied. Fig. 8(a) shows the speed tracking error ε_ω^* without load torque compensation. Fig. 8(b) shows the speed tracking error when the proposed load torque compensation is used. As

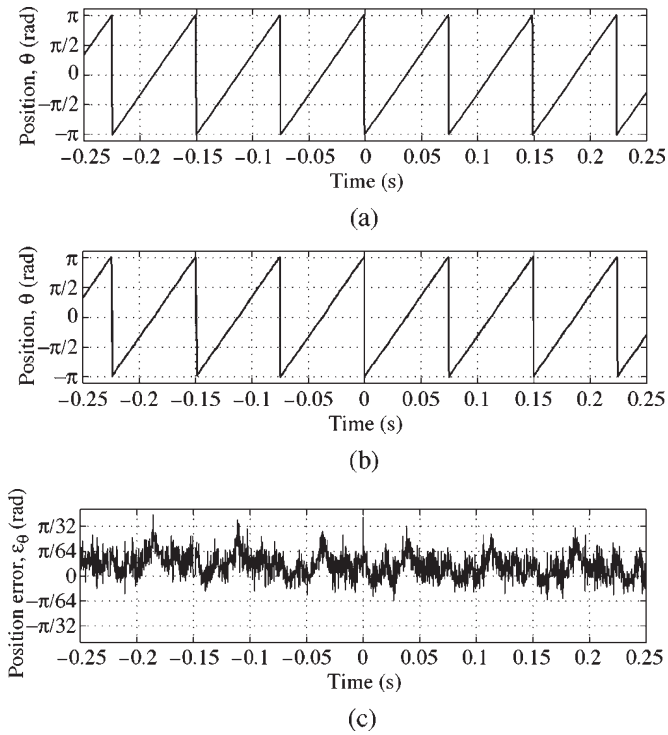

Fig. 7. Rotor position (in electrical radians) at low speed. (a) Measured θ. (b) Estimated $\widehat{\theta}$. (c) Estimation position error ε_θ.

can be seen, an improvement of almost 75% is obtained in the transient performance and also in the steady-state error. The estimated load torque can be seen in Fig. 8(c).

Fig. 9 shows the performance of the proposed sensorless control strategy under a regenerative load. Fig. 9(a) shows the speed tracking error, while the estimated load torque is presented in Fig. 9(b) when a -7-N·m load torque is applied. It can be seen that the estimated load torque is noisy in the regenerative region due to the influence of the chopped current of the braking unit.

A speed reversal test is presented in Fig. 10. The motor speed, when its reference is changed from 400 to -400 r/min, is shown

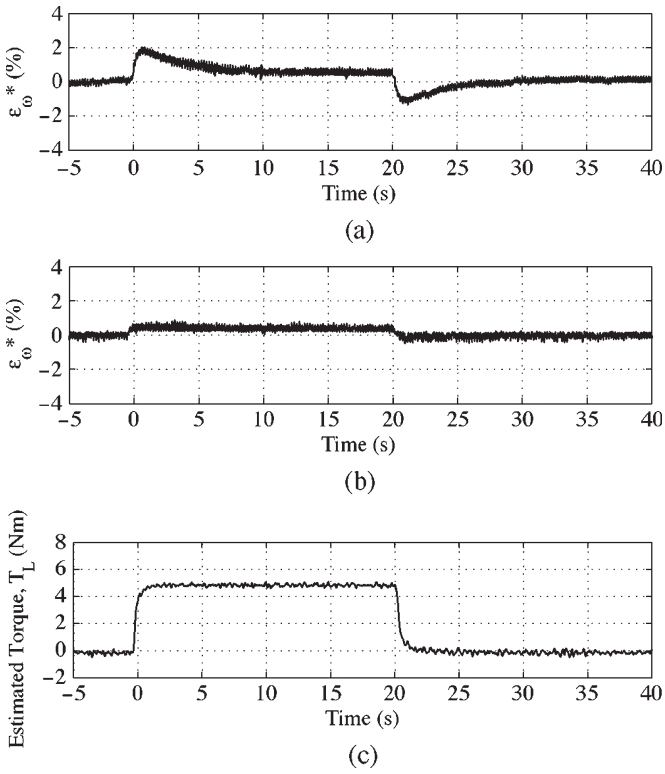

Fig. 8. Experimental results. Speed tracking error ε_ω^* (a) without load torque compensation; (b) with load torque compensation; and (c) with estimated load torque $\widehat{T}_L$.

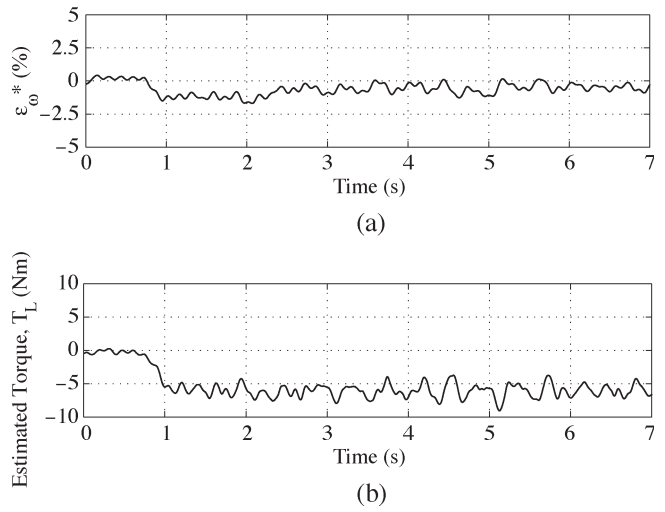

Fig. 9. Experimental results. Regenerative load. (a) Speed tracking error ε_ω^* and (b) estimated load torque $\widehat{T}_L$.

in this figure. It must be noted that the proposed observer cannot be used at very low or zero speed, just like other proposals based on the estimation of the induced EMF. However, a slight change is included in the algorithm to ensure its proper operation during speed reversal. This change consists of an open loop procedure, which allows the motor to reach the zero speed and start in the opposite direction [15]. If a sustained low-speed or standstill operation is needed, then the proposed observer should be combined with some signal injection techniques, as proposed in [16].

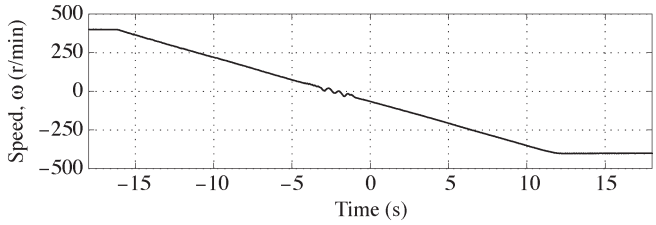

Fig. 10. Experimental results. Speed reversal test. Measured speed ω.

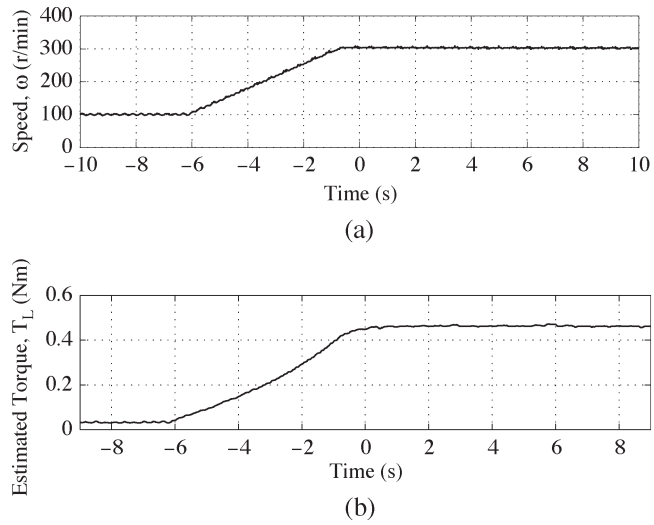

Fig. 11. Experimental results. Estimation of viscosity $B\omega$. (a) Machine speed ω and (b) estimated load torque $\widehat{T}_L$.

Finally, the estimation of perturbation $B\omega$ is shown in Fig. 11. Fig. 11(a) shows the machine's speed, when it is driven unloaded from 100 to 300 r/min. The estimation of $B\omega$ is shown in Fig. 11(b).

V. Conclusion

In this paper, a sensorless speed control strategy for high-performance PMACM drives with arbitrary EMF waveforms, using an extended nonlinear reduced-order observer, has been proposed. In order to improve the PMACM drive performance, the unknown disturbance torque is estimated by means of an adaptive law and is incorporated as a feedforward signal into the control loop.

A nonlinear reduced-order observer in combination with a load torque estimator presents two main advantages. One advantage is the improvement of the observer transient performance in comparison with a nonlinear full-order observer. The other advantage is the decrease in the steady-state EMF estimation error due to the use of the unknown load torque estimator.

The proposed observer includes information about the waveform of the induced EMF, which can be neither sinusoidal nor trapezoidal. Therefore, the proposed PMACM control scheme yields to a sensorless motor drive with minimum torque ripple and copper losses. Simulation and experimental results demonstrate the better performance of the proposed strategy over a conventional one, when an unknown load is applied.

APPENDIX
ADAPTATION LAW FOR LOAD TORQUE ESTIMATION AND WHOLE SYSTEM STABILITY

The adaptation law (10) can be designed as follows. The estimation errors are defined as

$$\varepsilon_e = \begin{bmatrix} \varepsilon_\alpha \\ \varepsilon_\beta \end{bmatrix} = \begin{bmatrix} e_\alpha - \widehat{e}_\alpha \\ e_\beta - \widehat{e}_\beta \end{bmatrix} \tag{26}$$

$$\varepsilon_{T_L} = T_L - \widehat{T}_L. \tag{27}$$

Then, the estimation-error dynamics will be given by

$$\begin{aligned} \frac{d\varepsilon_e}{dt} &= (\rho - \widehat{\rho}) - \frac{1}{J}\left(\varphi T_L - \widehat{\varphi}\widehat{T}_L\right) - g\varepsilon_e \\ \frac{d\varepsilon_{T_L}}{dt} &= -\,l_a \end{aligned} \tag{28}$$

where

$$\varphi = \begin{bmatrix} \varphi_\alpha \\ \varphi_\beta \end{bmatrix} \qquad \widehat{\varphi} = \begin{bmatrix} \widehat{\varphi}_\alpha \\ \widehat{\varphi}_\beta \end{bmatrix}$$

and

$$\rho = \begin{bmatrix} \frac{d\varphi_\alpha}{dt}\sqrt{\frac{e_\alpha^2+e_\beta^2}{\varphi_\alpha^2+\varphi_\beta^2}} + \frac{1}{J}\varphi_\alpha(\varphi_\alpha i_\alpha + \varphi_\beta i_\beta) \\ \frac{d\varphi_\beta}{dt}\sqrt{\frac{e_\alpha^2+e_\beta^2}{\varphi_\alpha^2+\varphi_\beta^2}} + \frac{1}{J}\varphi_\beta(\varphi_\alpha i_\alpha + \varphi_\beta i_\beta) \end{bmatrix}.$$

Note that ρ is a function of the induced EMF, the stator currents, and the function φ and its derivative. Taking into account (23) and (24), φ is also a function of the EMF through the rotor position given in (18). The estimation error in ρ ($\Delta\rho = \rho - \widehat{\rho}$) and φ ($\Delta\varphi = \varphi - \widehat{\varphi}$) is determined by the estimation error in the induced EMF (ε_e). Then, if the estimated EMF tends to the actual value, the estimates in ρ and φ does the same. Thus, it is possible to find a linear bound to their estimation errors given by

$$\begin{aligned} \|\Delta\rho\| &\le L_\rho\|\varepsilon_e\| \\ \|\Delta\varphi\| &\le L_\varphi\|\varepsilon_e\| \end{aligned} \tag{29}$$

where L_ρ and L_φ are $\Delta\rho$ and $\Delta\varphi$ Lipschitz constants, respectively. These constants can be calculated using, for example, the mean value theorem for multivariable functions or other real analysis tools. The reader interested in this subject is referred to [17].

To design the nonlinear expression l_a, the following Lyapunov candidate function is proposed:

$$V = \varepsilon_e^T\mathbf{P}\varepsilon_e + \Gamma^{-1}\varepsilon_{T_L}^2 \tag{30}$$

where $\mathbf{P}$ is a positive-definite matrix. Thus

$$\begin{aligned} \frac{dV}{dt} = -2g\varepsilon_e^T\mathbf{P}\varepsilon_e + 2\left(\Delta\rho^T - \frac{1}{J}T_L\Delta\varphi^T\right)\mathbf{P}\varepsilon_e \\ -\frac{2}{J}\varepsilon_{T_L}\widehat{\varphi}^T\mathbf{P}\varepsilon_e - 2\Gamma^{-1}\varepsilon_{T_L}l_a. \end{aligned} \tag{31}$$

The adaptation law (l_a) can be chosen in such a way to cancel the last two terms in (31)

$$-\frac{2}{J}\varepsilon_{T_L}\widehat{\varphi}^T\mathbf{P}\varepsilon_e - 2\Gamma^{-1}\varepsilon_{T_L}l_a = 0. \tag{32}$$

Then,

$$l_a = -\frac{\Gamma}{J}\widehat{\varphi}^T\mathbf{P}\varepsilon_e. \tag{33}$$

Therefore, the time derivative of the Lyapunov candidate function is rewritten as

$$\frac{dV}{dt} = -2g\varepsilon_e^T\mathbf{P}\varepsilon_e + 2\left(\Delta\rho^T - \frac{1}{J}T_L\Delta\varphi^T\right)\mathbf{P}\varepsilon_e. \tag{34}$$

Since $\Delta\rho$ and $\Delta\varphi$ are bounded by the Lipschitz constants indicated in (29) and the unknown load torque is assumed bounded ($\|T_L\| \le \gamma^*$), then a bound to the time derivative of the Lyapunov function is given by

$$\frac{dV}{dt} \le -2g\lambda_{\min}^{\mathbf{P}}\|\varepsilon_e\|^2 + (2L_\rho + 2\gamma L_\varphi)\lambda_{\max}^{\mathbf{P}}\|\varepsilon_e\|^2 \tag{35}$$

where $\gamma = \gamma^*/J$, and $\lambda_{\min}^{\mathbf{P}}$ and $\lambda_{\max}^{\mathbf{P}}$ are the minimum and maximum eigenvalues of the $\mathbf{P}$ matrix, respectively. Then, g must be chosen for guaranteeing a negative value of the right-hand side in (35), more details can be found in [5] and the references therein. As a consequence, the following inequality must be satisfied:

$$g > (L_\rho + \gamma L_\varphi)\left(\frac{\lambda_{\max}^{\mathbf{P}}}{\lambda_{\min}^{\mathbf{P}}}\right). \tag{36}$$

As previously mentioned, the observer can be designed for guaranteeing that the estimation error converges to zero. Then, the estimated values are to be used in a control law. It must be noted that a stable whole system can be obtained when controller parameters set are adequately chosen. A procedure for calculating the controller parameters when a nonlinear controller, a nonlinear observer, and a nonlinear plant are interconnected can be found in [18].

REFERENCES

[1] M. Iwasaki and N. Matsui, "Robust speed control of IM with torque feedforward control," *IEEE Trans. Ind. Electron.*, vol. 40, no. 6, pp. 553–560, Dec. 1993.

[2] G. Buja, R. Menis, and M. I. Valla, "Disturbance torque estimation in a sensorless DC drive," *IEEE Trans. Ind. Electron.*, vol. 42, no. 4, pp. 351–357, Aug. 1995.

[3] G. Zhu, L.-A. Dessaint, O. Akhrif, and A. Kaddouri, "Speed tracking control of a permanent-magnet synchronous motor with state and load torque observer," *IEEE Trans. Ind. Electron.*, vol. 47, no. 2, pp. 346–355, Apr. 2000.

[4] K.-H. Kim and M.-J. Youn, "A nonlinear speed control for a PM synchronous motor using a simple disturbance estimation technique," *IEEE Trans. Ind. Electron.*, vol. 49, no. 3, pp. 524–535, Jun. 2002.

[5] J. Solsona, M. I. Valla, and C. Muravchik, "Nonlinear control of a permanent magnet synchronous motor with disturbance torque estimation," *IEEE Trans. Energy Convers.*, vol. 15, no. 2, pp. 163–168, Jun. 2000.

[6] T. Senjyu, T. Shingaki, and K. Uezato, "Sensorless vector control of synchronous reluctance motors with disturbance torque observer," *IEEE Trans. Ind. Electron.*, vol. 48, no. 2, pp. 402–407, Apr. 2001.
[7] Y.-C. Lin, L.-C. Fu, and C.-Y. Tsai, "Nonlinear sensorless indirect adaptive speed control of induction motor with unknown rotor resistance and load," in *Proc. ACC*, San Diego, CA, Jun. 1999, pp. 2168–2172.
[8] T. Jahns and W. Soong, "Pulsating torque minimization techniques for permanent magnet AC motor drives—A review," *IEEE Trans. Ind. Electron.*, vol. 43, no. 2, pp. 321–330, Apr. 1996.
[9] R. Krishnan, *Electric Motor Drives: Modeling, Analysis, and Control*. Upper Saddle River, NJ: Prentice-Hall, 2001.
[10] J. Holtz and L. Springob, "Identification and compensation of torque ripple in high-precision permanet magnet motor drives," *IEEE Trans. Ind. Electron.*, vol. 43, no. 2, pp. 309–320, Apr. 1996.
[11] C. De Angelo, G. Bossio, J. Solsona, G. Garcia, and M. I. Valla, "A rotor position and speed observer for permanent magnet motor with non sinusoidal EMF waveform," *IEEE Trans. Ind. Electron.*, vol. 52, no. 3, pp. 807–813, Jun. 2005.
[12] M. Degner and R. Lorenz, "Using multiple saliencies for the estimation of flux, position, and velocity in AC machines," *IEEE Trans. Ind. Appl.*, vol. 34, no. 5, pp. 1097–1104, Sep./Oct. 1998.
[13] R. Leidhold, G. García, and E. Watanabe, "PMAC Motor control strategy, based on the instantaneous active and reactive power, for ripple-torque and copper-losses minimization," in *Proc. IEEE IECON*, Nagoya, Japan, Oct. 22–28, 2000, vol. 2, pp. 1401–1405.
[14] H. Akagi, Y. Kanazawa, and A. Nabae, "Generalized theory of the instantaneous reactive power in three-phase circuits," in *Proc. IPEC*, Tokyo, Japan, 1983, pp. 1375–1386.
[15] G. Zhu, A. Kaddouri, L.-A. Dessaint, and O. Akhrif, "A nonlinear state observer for the sensorless control of a permanent-magnet AC machine," *IEEE Trans. Ind. Electron.*, vol. 48, no. 6, pp. 1098–1108, Dec. 2001.
[16] M. Linke, R. Kennel, and J. Holtz, "Sensorless speed and position control of synchronous machines using alternating carrier injection," in *Proc. IEEE IEMDC*, Jun. 2003, vol. 2, pp. 1211–1217.
[17] H. K. Khalil, *Nonlinear Systems*, 2nd ed. Upper Saddle River, NJ: Prentice-Hall, 1996.
[18] M. Etchechoury, J. Solsona, and C. Muravchik, "Feedback linearization via state transformation using estimated states," *Int. J. Syst. Sci.*, vol. 32, no. 1, pp. 1–7, Jan. 2001.

Cristian De Angelo (S'96–M'05) received the Electrical Engineer degree from the Universidad Nacional de Río Cuarto (UNRC), Rio Cuarto, Argentina, and the Doctor of Engineering degree from the Universidad Nacional de La Plata (UNLP), La Plata, Argentina, in 1999 and 2004, respectively.

In 1994, he joined the Grupo de Electrónica Aplicada, UNRC. He is also currently with the Consejo Nacional de Investigaciones Científicas y Técnicas (CONICET), Argentina. His research interests include power electronics, sensorless motor control, electric vehicles, and renewable energy generation.

Dr. De Angelo is a member of the Automatic Control Association of Argentina.

Guillermo Bossio received the Electrical Engineer degree from the Universidad Nacional de Río Cuarto (UNRC), Río Cuarto, Argentina, and the Doctor of Engineering degree from the Universidad Nacional de La Plata (UNLP), La Plata, Argentina, in 1999 and 2004, respectively.

In 1994, he joined the Grupo de Electrónica Aplicada, UNRC. He is also currently with the Consejo Nacional de Investigaciones Científicas y Técnicas (CONICET), Argentina. His research interests include power electronics, sensorless motor control, electric vehicles, and renewable energy generation.

Dr. Bossio is a member of the Automatic Control Association of Argentina.

Jorge Solsona (S'94–A'95–M'97–SM'04) received the Electronics Engineer and Doctor of Engineering degrees from the Universidad Nacional de La Plata (UNLP), La Plata, Argentina, in 1986 and 1995, respectively.

From 1987 to 1997, he was a member of the Industrial Electronics, Control and Instrumentation Laboratory, Departamento de Electrotecnia, Facultad de Ingeniería, UNLP. From 1997 to 2003, he was with the Departamento de Electrotecnia, Facultad de Ingeniería, Universidad Nacional del Comahue. He is currently with the Instituto de Investigaciones en Ingeniería Eléctrica "Alfredo Desages," Departamento de Ingeniería Eléctrica y Computadoras, Universidad Nacional del Sur, Bahía Blanca, Argentina, and the Consejo Nacional de Investigaciones Científicas y Técnicas (CONICET), Argentina. He is involved in teaching and research on control theory and its applications to electromechanical systems.

Dr. Solsona is a member of the Automatic Control Association of Argentina.

Guillermo O. García (M'86–SM'01) received the Electrical and Electronics Engineering degree from the Universidad Nacional de Córdoba, Córdoba, Argentina, and the M.Sc. and Ph.D. degrees in electrical engineering from COPPE, Universidade Federal do Rio de Janeiro, Rio de Janeiro, Brazil, in 1981, 1990, and 1994, respectively.

In 1994, he joined the Universidad Nacional de Río Cuarto (UNRC), Río Cuarto, Argentina. He is currently the Director of the Grupo de Electrónica Aplicada, the Coordinator of a Graduate Program in electrical engineering, and a Professor in the Electrical and Electronics Department, UNRC. He is also with the Consejo Nacional de Investigaciones Científicas y Técnicas (CONICET), Argentina. His research interests include power electronics, motion control, electric vehicles, and renewable energy conversion.

Dr. García is a member of the Automatic Control Association of Argentina.

María Inés Valla (S'79–M'80–SM'97) received the Electronics Engineering and Doctor of Engineering degrees from the National University of La Plata (UNLP), La Plata, Argentina, in 1980 and 1994, respectively.

She is currently a Full Professor in the Electrical Engineering Department, Engineering Faculty, UNLP. She is also with the Consejo Nacional de Investigaciones Científicas y Técnicas (CONICET). She is engaged in teaching and research in the area of power converters and ac motor drives.

Dr. Valla is a Senior Member of the Administrative Committee of the IEEE Industrial Electronics Society (IES) and the IES Coordinator of Membership for Region 9. She has been a member of the organizing committees of several international conferences. She is also member of the Automatic Control Association of Argentina.